ACS APPLIED MATERIALS & INTERFACES

Letter

www.acsami.org

Nanoporous Carbon Sensor with Cage-in-Fiber Structure: Highly Selective Aniline Adsorbent toward Cancer Risk Management

Yasuhiro Kosaki,[†] Hironori Izawa,*[,‡,§,⊥] Shinsuke Ishihara,*[,‡] Kohsaku Kawakami,[‡] Masato Sumita,[‡] Yoshitaka Tateyama,[‡] Qingmin Ji,[‡] Venkata Krishnan,[‡,⊥] Shunichi Hishita,[‡] Yusuke Yamauchi,[‡] Jonathan P. Hill,[‡,§] Ajayan Vinu,*[,#] Seimei Shiratori,*[,†] and Katsuhiko Ariga*[,‡,§]

[†]Graduate School of Science and Technology, Keio University, 3-14-1, Hiyoshi, Kouhoku-ku, Yokohama 223-8522, Japan

[‡]International Center for Materials Nanoarchitectonics, National Institute for Materials Science, 1-1 Namiki, Tsukuba, Ibaraki 305-0044, Japan

[§]Japan Science and Technology Agency (JST), Core Research for Evolutional Science and Technology (CREST), 1-1 Namiki, Tsukuba, Ibaraki 305-0044, Japan

[#]Austrian Institute for Bioengineering & Nanotechnology, The University of Queensland, Brisbane 4072, Queensland, Australia

Supporting Information

ABSTRACT: Carbon nanocage-embedded nanofibrous film works as a highly selective adsorbent of carcinogen aromatic amines. By using quartz crystal microbalance techniques, even ppm levels of aniline can be repetitively detected, while other chemical compounds such as water, ammonia, and benzene give negligible responses. This technique should be applicable for high-throughput cancer risk management.

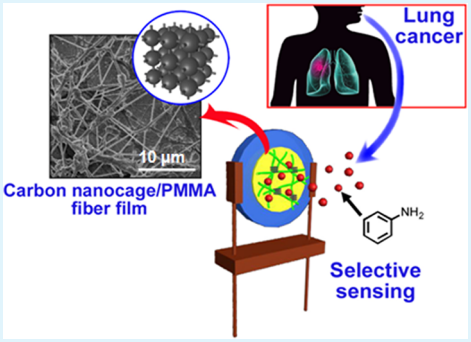

KEYWORDS: *carbons, mesoporous materials, quartz crystal microbalance, adsorption, sensors*

If lung cancer is detected in patients at an early enough stage a complete remission of the disease is possible after proper treatment.[1] However, most detection methods are expensive and time-consuming. Thus, apart from those who are lucky enough that their cancer is detected early (only 20%[2]), the lives of over million people are claimed by this disease every year.[3,4] To overcome this issue, the development of an easily implemented and cost-effective screening procedure for potential lung-cancer patients (i.e., tobacco users, workers in certain industries, etc.) is required.

Aromatic amines contained in cigarette smoke, broiled meats, some vegetables, and emissions from industries are structurally related carcinogens.[5] Daily exposure to aromatic amines increases the risk of their uptake,[6] in turn increasing the risk of contracting occupation-related cancers.[7] In fact, aromatic amines such as aniline and toluidines are found in excretia (exhaled breath[6] and urine.[8,9]) of most smokers. Aromatic amines can also be occasionally detected in nonsmoking lung cancer patients.[6] This is probably exogenous in origin and likely one of the causative substances.[10] Therefore, detection of volatile aromatic amines by breath gas analysis might reveal potential lung cancer patients. Although organic amines can be precisely and quantitatively detected by gas chromatographic analysis[6] or other sensing systems,[11−17] facile and high throughput methods applicable for detection of trace aromatic amines are uncommon.

Porous materials have been used for sensing applications because of their large adsorption capacities and good substrate selectivities.[18−29] However, the porous material showing good selectivity only to aromatic amine is rare. Here we report that carbon nanocage (CNC) exhibits highly selective adsorption for the aromatic-amine, aniline, and can be appliacble as higly selective aniline senor when subtle variation of mass upon adsorption is detected by quartz crystal microbalance (QCM) technique.[30−32] CNC is a mesoporous carbon material synthesized by using cage-type mesoporous silica KIT-5 as a template.[33−38] CNC has a cage-type structure possessing much greater surface area (1600 $m^2\ g^{-1}$) and pore volume (2.10 $cm^3\ g^{-1}$) than those reported for conventional mesoporous carbons.

To immobilize CNC onto a QCM electrode, a cast film of poly(methyl methacrylate) (PMMA) containing CNC (CNC/PMMA cast film) was fabricated by solvent-casting of an N,N-dimethylformamide (DMF) solution containing 0.10 wt % CNC and 0.15 wt % PMMA. For comparison, an activated

Received: March 14, 2013
Accepted: April 10, 2013
Published: April 10, 2013

   dx.doi.org/10.1021/am400940q | ACS Appl. Mater. Interfaces 2013, 5, 2930−2934

carbon (AC) embedded PMMA cast film (AC/PMMA cast film) was also fabricated. Subsequently, weights of sensing films were adjusted to ca. 1750 ng. SEM images show that CNC and AC particles are homogeneously dispersed in the cast films (see Figure S9a-b in the Supporting Information). QCM responses of the fabricated films toward aniline were evaluated by using a gas reservoir (i.e., a closed box) unit that enables simplified evaluation. Response (Hz) toward 3−12 ppm of aniline was plotted to estimate the slope (Hz/ppm) which represents the so-called response constant (R). Figure 1b shows R values of

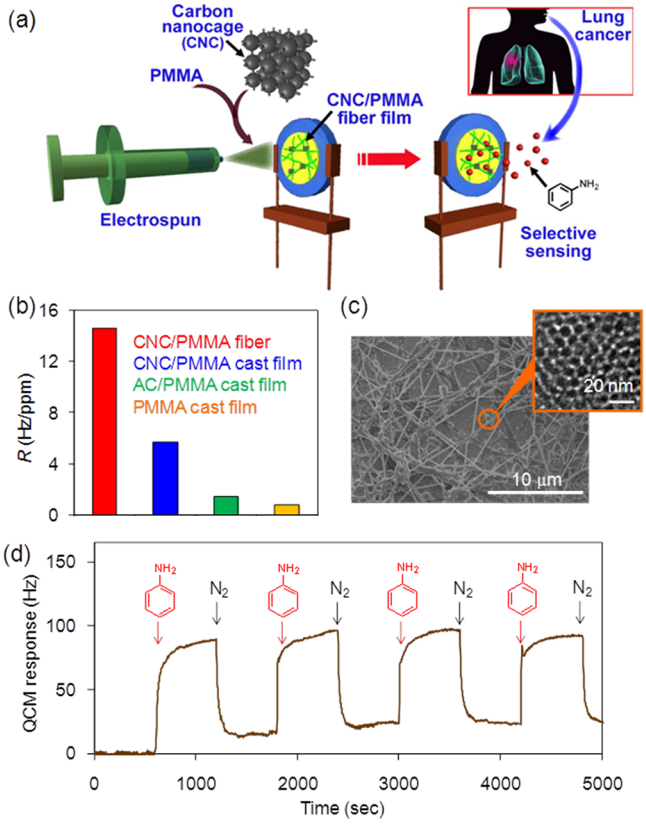

Figure 1. (a) Schematic illustration of this study. Highly sensitive aniline sensor by means of CNC and QCM technique. (b) Response constant (R) of each film to aniline vapor estimated from the slope of the QCM frequency shift in the range of 3−12 ppm aniline vapor. (c) SEM image of CNC-containing PMMA nanofiber film. The inset shows a high-resolution TEM image of CNC. (d) Repeating QCM response of CNC/PMMA fiber film for alternative exposure to aniline (7 ppm) and dry N_2 at 300 K.

the sensor toward aniline. The R value of CNC/PMMA film was 5.7 Hz/ppm, which is about 4 times greater than that of the AC/PMMA film. This is probably due to the chemical structure as is described below and the higher specific surface area of CNC.

To further enhance sensitivity, electrospun nanofibrous film containing CNC (CNC/PMMA fiber film) was studied since electrospun nanofibers offer a greater surface area and a porous membrane structure that are suitable for sensitive and rapid sensing.[39,40] These features have been shown to improved sensitivities over conventional materials in applications such as gas sensors, chemical sensors, optical sensors, and biosensors. The nanofibrous film was fabricated by optimized electrospinning from a DMF/THF (7/3) solution containing 10.0 wt % PMMA and 7.0 wt % CNC. Figure 1c shows an SEM image of the CNC/PMMA fiber film indicating incorporation of CNC within PMMA nanofibers. Note that CNC was thoroughly milled with mortar prior to electrospinning in order that it was roughly the same diameter as the nanofiber. As expected, the response of the CNC/PMMA fiber film was enhanced to 14.6 Hz/ppm (Figure 1b), which is ∼2.6 times greater than that of the cast film. Aniline can be easily desorbed from the CNC/PMMA fiber film by treating with dry N_2 flow, and repeatability of aniline sensing by the fiber film is also illustrated (Figure 1d).

To investigate selectivity for aniline, we studied R values of the CNC/PMMA fiber film for various volatile organic compounds (VOC) by using a gas flow unit (Figure 2a).

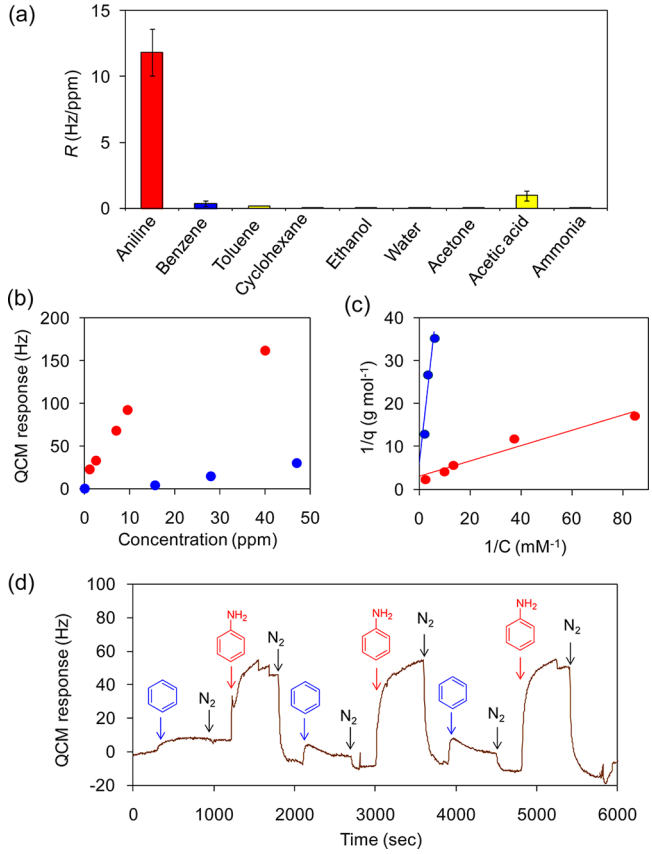

Figure 2. (a) R values of the CNC/PMMA fiber film for various volatile organic compounds. (b) QCM response (adsorption isotherms) of CNC/PMMA fiber film for aniline and benzene in the range of 0−50 ppm. (c) Langmuir plots of the adsorption isotherms of CNC/PMMA fiber film for anilin and benzene. (d) Repeating QCM response of CNC/PMMA fiber film for alternative exposure to aniline (5 ppm) and benzene (13 ppm) vapors. Note that sudden decrease in QCM response was observed at around 1500 and 5200 s, probably because of the partial removal of CNC/PMMA fiber from QCM electrode by N_2 stream.

Surprisingly, the R value for aniline was significantly greater than for the others. Of special note is that response values for benzene (0.2 Hz/ppm) and toluene (0.4 Hz/ppm) were substantially lower than that for aniline (11.9 Hz/ppm), although their bindings are able to be enhanced by $\pi-\pi$ interaction, which suggests the importance of hydrogen bonding with the amino group of aniline. However, the R value of ammonia gas was also low (0.1 Hz/ppm). These results suggest the presence of cooperative multiple points of interaction involving $\pi-\pi$ forces and hydrogen bonding

dx.doi.org/10.1021/am400940q | ACS Appl. Mater. Interfaces 2013, 5, 2930−2934

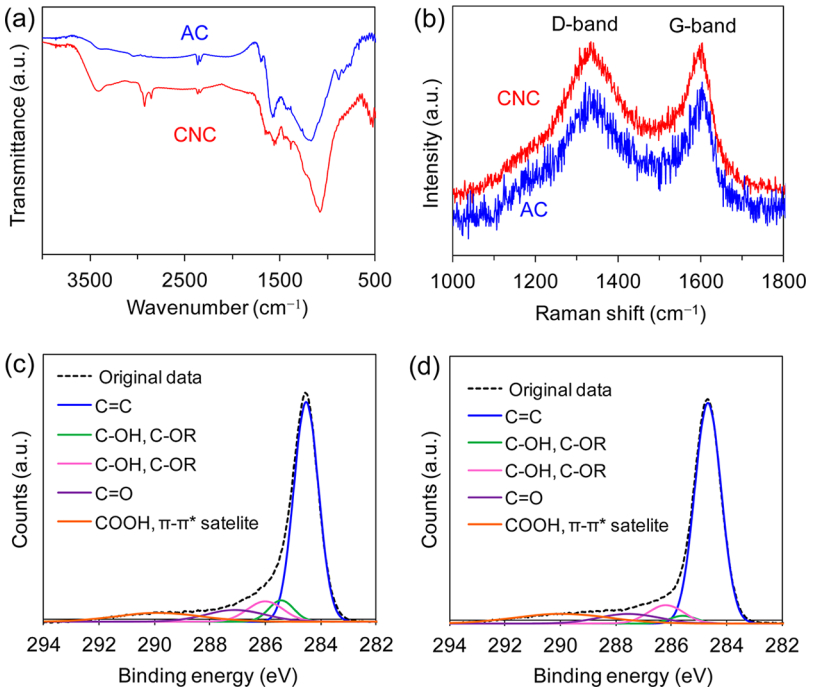

Figure 3. (a) IR spectrum of CNC and AC. (b) Raman spectrum of CNC and AC. (c) XPS of CNC in the region of C1s. (d) XPS of AC in the region of C1s.

between aniline and CNC. Figure 2b shows adsorption isotherms of aniline and benzene. Aniline is obviously much more strongly adsorbed when compared with benzene. Langmuir plots for these reveal that both benzene and aniline have a linear relationship of response, suggesting monolayer coverage of aniline or benzene. Binding constants (K) between aniline or benzene and CNC/PMMA fiber film, estimated from Langmuir plots were 1852.1 and 36.4 M^{-1}, respectively (Figure 2c). This large difference in their K values could be clearly demonstrated by alternate flow of benzene then aniline (Figure 2d), in which benzene (13 ppm) and aniline (5 ppm) were applied alternately for 10 min with an interval of 5 min. When volatile benzene was flowed at 5, 35, and 65 min, the frequency was increased by ca. 10 Hz. In contrast, when an approximately 3 times lower concentration of volatile aniline was flowed after 20, 50, 80 min, the frequency was increased by ca. 60 Hz.

To investigate the chemisorbed structure of CNC with aniline, we performed chemical analyses of CNC. Figure 3a shows IR spectra of CNC and AC. Two peaks at 1600 cm^{-1} and 1720 cm^{-1} correspond to carbonyl groups of carboxylic acids, lactones and/or acid anhydrides were observed. In the case of CNC, very broad band derived from O−H stretching of phenol was observed in the range 3200−3400 cm^{-1}.[41] In addition, distinct IR peaks observed at around 3000 cm^{-1} indicates that CNC contains C−H units, meaning the incomplete carboniation. Generally, carbonization degrees in products are controlled by changing mesoporous silica templates, carbonization temperatures, and carbon sources.[42−48] The carbonization degree of CNC is relatively low in comparison with other porous carbons reported previously,[42−48] but this point is critically important for selective aromatic-amine adsorbent (The details are given in the later section.). Figure 3b shows Raman spectra of CNC and AC. These spectra, reveal no significant difference between CNC and AC. In the Raman spectrum of CNC, the tangential G band around 1610 cm^{-1} and the defect-induced D band around 1345 cm^{-1} are present, indicating a substantial quantity of graphene sheets are contained in CNC. X-ray photoelectron spectroscopy (XPS) was used to further investigate the structure of CNC and AC (Figure 3c, d). XPS is a frequently used to investigate surface functionality of carbon materials and it enables detection of subtle chemical differences within 10−15 nm of the surface of the analyte.[49,50] The deconvoluted high-resolution C1s spectrum of AC is comprised of an intense peak at 284.7 eV from sp^2 (−C═C−) carbon accompanied with relatively weak peaks around 286−290 eV, which are typical of alcohol (−C−OH), carbonyl (C═O), and carboxyl (−COOH) carbons (see Table S1 in the Supporting Information).[49,50] CNC contains relatively more intense C1s peaks in the 286−290 eV region compared with AC. These results strongly suggest that CNC contains not only sp^2 carbons (i.e., aromatic units) but also a larger quantity of the previously mentioned alcohol, carbonyl and carboxyl functional groups, which has also been observed in other zeolite-templated microporous carbons reported by Kyotani et al.[41]

To obtain an insight into the highly selective adsorption of aniline by CNC, we investigated the chemisorbed structure of aniline with CNC by using density functional theory (DFT). As a simplified model structure of CNC, a partially segmented graphene nanosheet with various functional groups (i.e., carboxylic anhydride, ether, and phenol group) was designed in accord with the above results. Possible moieties that interact with aniline are C═O, O−H and π-orbitals of five or six membered rings. Hence, three aniline molecules were placed around the segmented graphene nanosheet, and then density functional molecular dynamics (DFMD) was applied (Figure 4a). We found that only a single aniline molecule interacts with a carbonyl group (C═O) remaining in the vicinity of the CNC model. We also constructed a model of the system of an interacting benzene and CNC model by replacing the interacting aniline with benzene. Geometry optimizations on the molecules of aniline and benzene interacting with the CNC

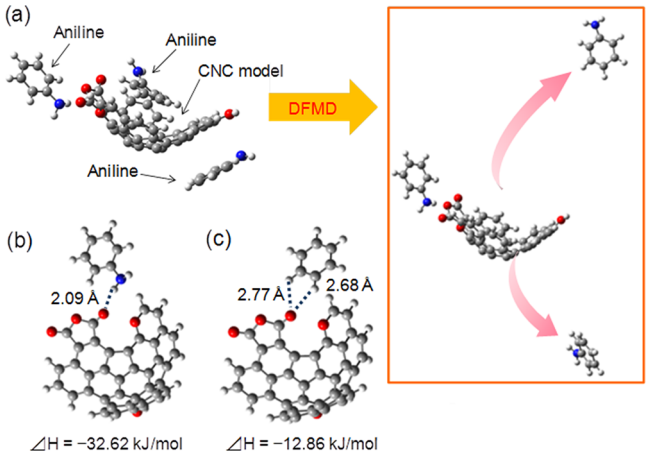

Figure 4. (a) Results of density functional molecular dynamics simulation (DFMD) at 300 K to determine possible location(s) of aniline molecules interacting with a CNC model. (b) Optimized strucure parameters of CNC-aniline complex at the B3LYP/6-31G* level. (c) Optimized strucure parameters of CNC-benzene complex at the B3LYP/6-31G* level.

model yield the different binding energies between aniline and benzene and the CNC model (Figure 4b, c). Estimated binding energy between benzene and the CNC model is 19.76 kJ mol^{-1} lower than that of aniline, which indicates that the benzene molecule interacts weakly with the carbonyl group (C═O) through CH−π interaction. This result also suggests that hydrogen bonding between amine group in aniline and carbonyl group in CNC is a crucial interaction for the selective adsorption of aniline by CNC. π−π interactions between the aromatic ring of aniline and the graphene nanosheet of the CNC model was not observed in our calculations most likely due to the limited fragment structure of our CNC model. However, various carbon-based adsorption materials are known to exhibit high affinity to aromatic molecules because of π−π interactions.[18] Thus, we believe that π−π interactions should exist between aniline and CNC and we suppose that the cooperativity between hydrogen bonding and π−π interactions should make CNC a highly selective adsorbent for aromatic amines such as aniline.

In conclusion, CNC-embedded nanofibrous film demonstrates highly selective adsorption selectivity for aromatic amines over water, benzene, ammonia and other chemical species, and even ppm levels of aniline can be detected by means of QCM sensing techniques. CNC-embedded nanofibrous film can be used repeatedly, so that facile, high throughput, low cost and quantitative detection techniques of volatile aromatic amines are possible. This could lead to cancer risk management by using breath gas analysis prior to contraction of cancer (or at an earlier stage of the disease) and assessment of aromatic amines in the workplace, leading to reducing mortality due to anthropogenic carcinogens. In addition, our method could be also used for the other nanostrucured materials[51−53] for sensitive sensors, removal of toxic compounds, and controlled-release system.

EXPERIMENTAL SECTION

Evaluation of Sensor Performance with the Gas Reservoir Unit. In a typical experiment, the gas sensor system was located in the gas reservoir unit (Figure S2). A high concentration of aniline vapor was injected by syringe causing variation in the concentration of aniline in the desiccator. Liquid aniline was warmed under dry N_2 until the vapor was saturated and the aniline-saturated vapor was collected in a Tedlar(R) bag. The collected vapor was applied immediately to the gas reservoir unit. Aniline concentration was measured by using an aniline gas detector tube (GASTEC No.181).

Evaluation of Sensor Performance with the Gas Flow Unit. The gas sensor system was connected to the gas flow unit (Figure S3) containing the aniline vapor in N_2 (or the other vapor for analysis) which was then flowed though the sensor chamber in the gas sensor system (see Figure S1 in the Supporting Information). Aniline-saturated vapor was mixed with dry N_2 in the flow line to regulate concentration. Note that in the case of ammonia gas, 210 ppm of ammonia gas from a cylinder was mixed directly with N_2. Concentrations of all vapors were measured using the respective gas tube detector (GASTEC).

ASSOCIATED CONTENT

Supporting Information

Material, experimental setup, SEM images, XPS results, and computational details. This material is available free of charge via the Internet at http://pubs.acs.org.

AUTHOR INFORMATION

Corresponding Author

*E-mail: ARIGA.Katsuhiko@nims.go.jp.

Present Address

⊥H.I. is currently at Graduate School of Engineering, Department of Chemistry and Biotechnology, Tottori University, 4−101, Koyamachominami, Tottori-shi, Tottori 680−8552, Japan. V.K. is currently at the School of Basic Sciences, Indian Institute of Technology Mandi, Mandi 175−001, Himachal Pradesh, India.

Notes

The authors declare no competing financial interest.

ACKNOWLEDGMENTS

This research was partially supported by the World Premier International Research Center Initiative on Materials Nanoarchitectonics from MEXT (Japan), KAKENHI 25810055 from JSPS (Japan), CREST-project, PRESTO-project from JST (Japan). Theoretical study was partly supported by KAKENHI 20540384 and 23340089 as well as the Strategic Programs for Innovative Research (SPIRE), MEXT and the Computational Materials Science Initiative (CMSI), Japan. The calculations in this work were carried out on the supercomputer centers of NIMS, ISSP, The University of Tokyo, T2K-Tokyo, and T2K-Tsukuba.

REFERENCES

(1) Cassidy, A.; Duffy, S. W.; Myles, J. P.; Liloglou, T.; Field, J. K. *Int. J. Cancer* **2006**, *120*, 1−6.
(2) Ellis, J. R. C.; Gleeson, F. V. *Brit. J. Radiol.* **2001**, *74*, 478−485.
(3) Spiro, S. G.; Tanner, N. T.; Silvestri, G. A.; Janes, S. M.; Lim, E.; Vansteenkiste, J. F.; Pirker, R. *Respirology* **2010**, *15*, 44−50.
(4) Spiro, S. G.; Silvestri, G. A. *Am. J. Resp. Crit. Care* **2005**, *172*, 523−529.
(5) Turesky, R. J.; Le Marchand, L. *Chem. Res. Toxicol.* **2011**, *24*, 1169−1214.
(6) Preti, G.; Labows, J. N.; Kostelc, J. G.; Aldinger, S.; Daniele, R. *J. Chromatogr.−Biomed.* **1988**, *432*, 1−11.

(7) Pira, E.; Piolatto, G.; Negri, E.; Romano, C.; Boffetta, P.; Lipworth, L.; McLaughlin, J. K.; La Vecchia, C. *J. Natl. Cancer Inst.* **2010**, *102*, 1096−1099.
(8) Freudenthal, R. I.; Anderson, D. P. *J. Natl. Cancer Inst.* **1997**, *89*, 734.
(9) Elbayoumy, K.; Donahue, J. M.; Hecht, S. S.; Hoffmann, D. A. *Cancer Res.* **1986**, *46*, 6064−6067.
(10) Filipiak, W.; Sponring, A.; Mikoviny, T.; Ager, C.; Schubert, J.; Miekisch, W.; Amann, A.; Troppmair., J. *Cancer Cell Int.* **2008**, *8*, 17.
(11) Che, Y. K.; Zang, L. *Chem. Commun.* **2009**, 5106−5108.
(12) Gao, T.; Tillman, E. S.; Lewis, N. S. *Chem. Mater.* **2005**, *17*, 2904−2911.
(13) Jiang, B. P.; Guo, D. S.; Liu, Y. *J. Org. Chem.* **2011**, *76*, 6101−6107.
(14) Liu, X.; Zhang, X.; Lu, R.; Xue, P.; Xu, D.; Zhou, H. *J. Mater. Chem.* **2011**, *21*, 8756−8765.
(15) Raible, I.; Burghard, M.; Schlecht, U.; Yasuda, A.; Vossmeyer, T. *Sens. Actuaor, B* **2005**, *106*, 730−735.
(16) Sotzing, G. A.; Phend, J. N.; Grubbs, R. H.; Lewis, N. S. *Chem. Mater.* **2000**, *12*, 593−595.
(17) Tang, Z. L.; Yang, J. H.; Yu, J. Y.; Cui, B. *Sensors* **2010**, *10*, 6463−6476.
(18) Ariga, K.; Vinu, A.; Yamauchi, Y.; Ji, Q.; Hill, J. P. *Bull. Chem. Soc. Jpn.* **2012**, *85*, 1−32.
(19) Ariga, K.; Ji, Q.; McShane, M. J.; Lvov, Y. M.; Vinu, A.; Hill, J. P. *Chem. Mater.* **2012**, *24*, 728−737.
(20) Zhang, J.; Chang, M. *Chem. Soc. Rev.* **2012**, *41*, 7016−7031.
(21) Kreno, L. E.; Leong, K.; Farha, O. K.; Allendorf, M.; Van Duyne, R. P.; Hupp, J. T. *Chem. Rev.* **2012**, *112*, 1105−1125.
(22) Tsang, C. K.; Kelly, T. L.; Sailor, M. J.; Li, Y. Y. *ACS Nano* **2012**, *6*, 10546−10554.
(23) Brutschy, M.; Schneider, M. W.; Mastalerz, M.; Waldvogel, S. R. *Adv. Mater.* **2012**, *24*, 6049−6052.
(24) Wang, F.; Zhao, J. B.; Gong, J. M.; Wen, L. L.; Zhou, L.; Li, D. F. *Chem.—Eur. J.* **2012**, *18*, 11804−11810.
(25) Wanderley, M. M.; Wang, C.; Wu, C. D.; Lin, W. B. *J. Am. Chem. Soc.* **2012**, *134*, 9050−9053.
(26) Wu, P. Y.; Wang, J.; He, C.; Zhang, X. L.; Wang, Y. T.; Liu, T.; Duan, C. Y. *Adv. Funct. Mater.* **2012**, *22*, 1698−1703.
(27) Kimura, M.; Sakai, R.; Sato, S.; Fukawa, T.; Ikehara, T.; Maeda, R.; Mihara, T. *Adv. Funct. Mater.* **2012**, *22*, 469−476.
(28) Lu, Z.-Z.; Zhang, R.; Li, Y.-Z.; Guo, Z.-J.; Zheng, H.-G. *J. Am. Chem. Soc.* **2011**, *133*, 4172−4174.
(29) Takashima, Y.; Martinez, V. M.; Furukawa, S.; Kondo, M.; Shimomura, S.; Uehara, H.; Nakahama, M.; Sugimoto, K.; Kitagawa, S. *Nat. Commun.* **2011**, *2*, 168.
(30) Ji, Q.; Yoon, S. B.; Hill, J. P.; Vinu, A.; Yu, J.-S.; Ariga, K. *J. Am. Chem. Soc.* **2009**, *131*, 4220−4221.
(31) Mane, G. P.; Talapaneni, S. N.; Anand, C.; Varghese, S.; Iwai, H.; Ji, Q.; Ariga, K.; Mori, T.; Vinu, A. *Adv. Funct. Mater.* **2012**, *22*, 3596−3604.
(32) Jia, L.; Mane, G. P.; Anand, C.; Dhawale, D. S.; Ji, Q.; Ariga, K.; Vinu, A. *Chem. Commun.* **2012**, *48*, 9029−9031.
(33) Ariga, K.; Vinu, A.; Miyahara, M.; Hill, J. P.; Mori, T. *J. Am. Chem. Soc.* **2007**, *129*, 11022−11023.
(34) Vinu, A.; Miyahara, M.; Mori, T.; Ariga, K. *J. Porous. Mater.* **2006**, *13*, 379−383.
(35) Vinu, A.; Miyahara, M.; Sivamurugan, V.; Mori, T.; Ariga, K. *J. Mater. Chem.* **2005**, *15*, 5122−5127.
(36) Vinu, A.; Mori, T.; Ariga, K. *Sci. Technol. Adv. Mater.* **2006**, *7*, 753−771.
(37) Datta, K. K. R.; Vinu, A.; Mandal, S.; Al-Deyab, S.; Hill, J. P.; Ariga, K. *J. Nanosci. Nanotechnol.* **2011**, *11*, 3959−3964.
(38) Datta, K. K. R.; Vinu, A.; Mandal, S.; Al-Deyab, S.; Hill, J. P.; Ariga, K. *J. Nanosci. Nanotechnol.* **2011**, *11*, 3084−3090.
(39) Hunley, M. T.; Long, T. E. *Polym. Int.* **2008**, *57*, 385−389.
(40) Di, J.; Zhao, Y.; Yu, J. *J. Mater. Chem.* **2011**, *21*, 8511−8520.
(41) Nishihara, H.; Yang, Q.-H.; Hou, P.-X.; Unno, M.; Yamauchi, S.; Saito, R.; Paredes, J. I.; Martínez-Alonso, A.; Tascón, J. M. D.; Sato, Y.; Terauchi, M.; Kyotani, T. *Carbon* **2009**, *47*, 1220−1230.
(42) Lee, J.; Kim, J.; Hyeon, T. *Adv. Mater.* **2006**, *18*, 2073−2094.
(43) Yuan, D. S.; Zeng, J.; Chen, J.; Liu, Y. *Int. J. Electrochem. Sci.* **2009**, *4*, 562−570.
(44) Wu, Z.; Li, W.; Xia, Y.; Webley, P.; Zhao, D. *J. Mater. Chem.* **2012**, *22*, 8835−8845.
(45) Sterk, L.; Górka, J.; Vinu, A.; Jaroniec, M. *Microporous Mesoporous Mater.* **2012**, *156*, 121−126.
(46) Wickramaratne, N. P.; Jaroniec, M. *Carbon* **2013**, *51*, 45−51.
(47) Górka, J.; Zawislak, A.; Choma, J.; Jaroniec, M. *Appl. Surf. Sci.* **2010**, *256*, 5187−5190.
(48) Poh, H. L.; Pumera, M. *Chem. Asian J.* **2012**, *7*, 412−416.
(49) Shen, W.; Li, Z.; Liu, Y. *Recent Patents on Chemical Engineering 1* **2008**, *1*, 27−40.
(50) Lascovich, J. C.; Giorgi, R.; Scaglione, S. *Appl. Surf. Sci.* **1991**, *47*, 17−21.
(51) Abdullayev, E.; Lvov, Y. *J Nanosci. Nanotechnol.* **2011**, *11*, 10007−10026.
(52) Vergaro, V.; Lvov, Y. M.; Leporatti, S. *Macromol. Biosci.* **2012**, *12*, 1265−1271.
(53) Abdullayev, E.; Price, R.; Shchukin, D.; Lvov, Y. *ACS Appl. Mater. Interfaces* **2009**, *1*, 1437−1443.